Accepted Manuscript

Antibiotic protected silver nanoparticles for microbicidal cotton

Ana Maria Montagut, Albert Granados, Anna Ballesteros, Roser Pleixats, Montserrat Llagostera, Pilar Cortés, Rosa María Sebastián, Adelina Vallribera

PII: S0040-4020(18)31375-9

DOI: https://doi.org/10.1016/j.tet.2018.11.035

Reference: TET 29946

To appear in: *Tetrahedron*

Received Date: 13 September 2018

Revised Date: 13 November 2018

Accepted Date: 15 November 2018

Please cite this article as: Montagut AM, Granados A, Ballesteros A, Pleixats R, Llagostera M, Cortés P, Sebastián RosaMarí, Vallribera A, Antibiotic protected silver nanoparticles for microbicidal cotton, *Tetrahedron* (2018), doi: https://doi.org/10.1016/j.tet.2018.11.035.

Graphical Abstract

To create your abstract, type over the instructions in the template box below.
Fonts or abstract dimensions should not be changed or altered.

Antibiotic protected silver nanoparticles for microbicidal cotton

Leave this area blank for abstract info.

Ana Maria Montagut,[a] Albert Granados,[a] Anna Ballesteros,[a] Roser Pleixats,[a] Montserrat Llagostera,[b] Pilar Cortés,[b,*] Rosa María Sebastián[a,*] and Adelina Vallribera[a,*]

[a]*Department of Chemistry and Centro de Innovación en Química Avanzada (ORFEO-CINQA), Universitat Autònoma de Barcelona, Cerdanyola del Vallès, 08193-Barcelona*

[b]*Department of Genetics and Microbiology, Universitat Autònoma de Barcelona, Cerdanyola del Vallès, 08193-Barcelona*

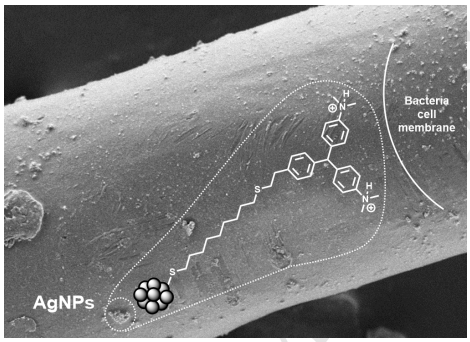

Tetrahedron
journal homepage: www.elsevier.com

Antibiotic protected silver nanoparticles for microbicidal cotton

Ana Maria Montagut,[a] Albert Granados,[a] Anna Ballesteros,[a] Roser Pleixats,[a] Montserrat Llagostera,[b] Pilar Cortés,[b,*] Rosa María Sebastián[a,*] and Adelina Vallribera[a,*]

[a] *Department of Chemistry and Centro de Innovación en Química Avanzada (ORFEO-CINQA), Universitat Autònoma de Barcelona, Cerdanyola del Vallès, 08193-Barcelona*
[b] *Department of Genetics and Microbiology, Universitat Autònoma de Barcelona, Cerdanyola del Vallès, 08193-Barcelona*

ARTICLE INFO

Article history:
Received
Received in revised form
Accepted
Available online

Keywords:
Bactericidal
Silver
Eugenol
Fluoroquinolone
PEG

ABSTRACT

Surface coating of metal nanoparticles is one of the major aspects to be optimized in the design of antimicrobial nanoparticles. The novelty of this work is that antimicrobial derivatives have been used as stabilizers to protect silver nanoparticles (Ag NPs). Microbicidal activity studies of fabricated cotton textiles coated with these Ag@Antibio were performed. Protective ligand layers of Ag NPs resulted to be a deterministic factor in their antimicrobial activity. The best bactericidal activity was obtained for **Fabric TAM** (coated with Ag NPs with triarylmethane derivates in surface, **Ag@TAMSH**), with a bacterial decrease of 3 log units for the *S. aureus* strain. Intrinsic antibiotic activity and partial positive charge of the **TAMSH** probably enhanced their antimicrobial effects. **Fabric Eu** (coated with Ag NPs with eugenol derivates in surface, **Ag@EugenolSH**) and **Fabric FQPEG** (coated with Ag NPs embedded in PEG-fluoroquinolone derivatives in surface, **Ag@FQPEG**) displayed antibacterial activity for both *Staphylococcus aureus* and *Pseudomonas aeruginosa* strains. These coated antimicrobial cotton fabrics can be applied in different medical textiles.

1. Introduction

Materials capable of fulfilling multiple functions simultaneously in time are of significance to improve the performance of products. Cotton is one of the most widely used natural fibers for textiles because of its breathability, softness and degradable nature. Cotton with enhanced functionalities such as self-cleaning,[1] flame retardation,[2] UV protection,[3] and antibacterial[4] is greatly appreciated by a demanding consumer market for high-value added products.

The efficiency of silver as an antibacterial agent has been known during centuries, and with the appearance of silver nanoparticles (Ag NPs) their use is growing sharply. Ag NPs are well known for their properties against a wide range of bacteria and fungi.[5] Thus, cotton fabrics have been endowed with antimicrobial function by coating with Ag NPs.[6] The efficiency increases with reduced size, because smaller particles have a larger surface area able to interact with microorganisms.[7] The main toxic proposed mechanism of NPs is thought to be the oxidative stress resulting in damage to the lipids, proteins and DNA of the microorganisms.[8] Ag NPs attack the respiratory chain cell division that finally lead to cell death, while concomitantly releasing silver ions that enhance bactericidal activity. Ag NPs would first accumulate on the surface of the bacterial membrane, then would penetrate into the bacteria, and finally would change the permeability of bacterial membrane causing a substantial damage. Owing to their characteristics they are nowadays one of the most commercialized types of nanomaterials, being present in more than 200 products. Moreover, Ag NPs display applications in different fields such as antimicrobial coatings, medical devices, textiles, home water purifiers, household appliances, among others.

The group of S. R. Joshi has described that formulations of Ag NPs with commonly used antibiotics such as penicillin G, amoxicillin, erythromycin and vancomycin resulted in enhanced and synergic antimicrobial effects against Gram-positive and Gram-negative bacteria (*S. aureus* and *E. coli*).[9] Having in mind this precedent, and the fact that Ag NPs usually require stabilizing agents to avoid their agglomeration, we envisaged the use of an antimicrobial active compound as stabilizer. The Ag NPs's physicochemical properties have a strong influence in the interaction between the nanoparticles and the bacterial membrane. These properties include surface charge, binding

tendency towards bacteria, and aggregation and dissolution potential. In particular, certain protecting ligand layers could better interact with the bacteria, resulting in high efficacy in damaging the bacterial membrane.

With the idea that surface coating of metal nanoparticles is one of the major aspects to be optimized in the design of antimicrobial Ag NPs, we describe here the preparation of silver nanoparticles using different antimicrobial derivatives as stabilizers. This approach is completely new and we want to explore if these Ag NPs present enhanced microbicidal properties when deposited on the surface of a cotton fabric. On one side, compounds bearing antibacterial properties, such as eugenol, triarylmethane and fluoroquinolone, have been conveniently functionalized with thiol groups to be used as stabilizers. On the other hand, we have prepared polyethylene glycol (PEG)-tagged antibiotics as confining polymers for the stabilization of silver nanoparticles. Coating of cotton fabrics with these silver-antibiotic nanoparticles (Ag@Antibio) is also reported, as well as the characterization of all the silver-based materials and their microbicidal activity.

2. Results and discussion

We describe first the preparation of Ag@Antibio. Taking advantage of our previous experience in the preparation of metal nanoparticles,[10] the synthesis of the Ag stabilizers was based on a derivatization strategy (thiol-ene reaction) applicable in all selected antibiotics. Prior modification of the original antibiotic to incorporate a thiol group was undertaken to take profit of the well-known silver-thiol affinity.[11] In addition, the length of the linker between the SH group and the antibiotic moiety ought to be appropriate for facile binding to the Ag nanoparticle, avoiding the steric hindrance of the active biological molecule in the surface. Moreover, given that the functional groups of the antibiotic may play a crucial rule in their bioactivity, the point of attachment of the thiol linker was carefully selected. Thus, we decided to incorporate a vinyl group on the antibiotic and then to carry out common thiol–ene coupling using nonane-1,9-dithiol.[12]

Eugenol **1** was first selected due to its known antibacterial properties and the presence of a double bound in the molecule.[13] The desired thiol-bearing eugenol **2** (EugenolSH) was prepared in 85% yield using 3 equiv. of nonane-1,9-dithiol in glycerol (Scheme 1). In this reaction, 10% of the compound corresponding to the double addition of the dithiol to two molecules of eugenol was also isolated (see supplementary information (S6)).

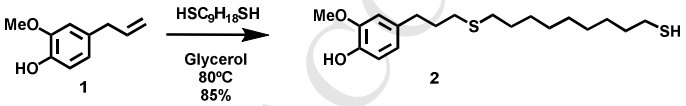

Scheme 1. Preparation of the stabilizer **2 (**EugenolSH**)**

Another family of antimicrobials is related to the known Malachite green, which is an extensively world-wide used biocide in the aquaculture industry.[14] Thus, we turn to the synthesis of the vinyl derivative **5** (Scheme 2). We carried out a palladium-catalyzed cross-coupling reaction of potassium vinyltrifluoroborate with 4-bromobenzaldehyde using 2 mol % $PdCl_2$/6 mol % of PPh_3 as catalyst, and Cs_2CO_3 as a base in a 9:1 mixture of THF/H_2O, affording 4-vinylbenzaldehyde, **4**, in 97% yield (Scheme 2).[15] The diaminotriarylmethane **5** was prepared (51% yield) through the Baeyer condensation of the aromatic aldehyde **4** and *N,N*-dimethylaniline in the presence of niobium chloride under solvent-free conditions.[16] Subsequent addition of nonane-1,9-dithiol in glycerol gave the desired thiol **6** (TAMSH) (22% yield). Other methodologies based on the use of AIBN as radical initiator were tested, but decomposition of **5** was observed in all cases, probably due to the quick formation of a reactive radical at the $CH(Ar)_3$ position.

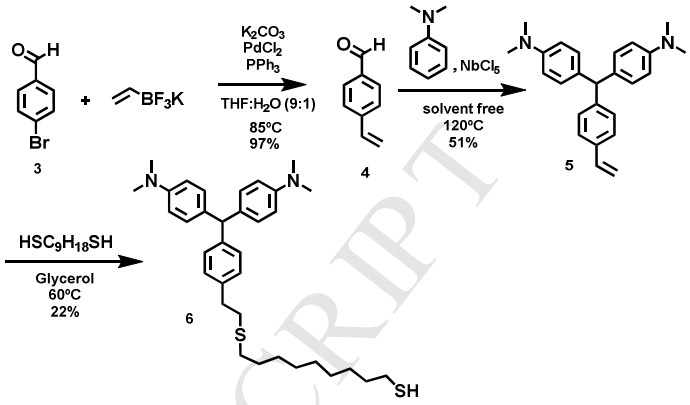

Scheme 2. Preparation of the stabilizer **6 (**TAMSH**)**

We then selected another well-known family of antibiotics, the fluoroquinolones.[17] Fluoroquinolone **7** was prepared following a methodology previously described by the group of H. Koga.[18] Subsequent addition of dithiol gave **8** in a moderate 35% yield. Acid hydrolysis of the ethyl ester afforded FQSH, **9**, in quantitative yield (Scheme 3).

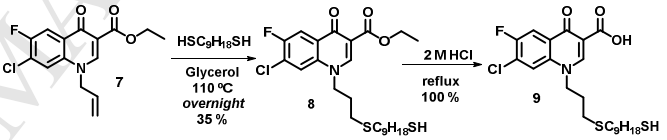

Scheme 3. Preparation of the stabilizer **9 (**FQSH**)**

With the thiol stabilizers in hand, we undertook the synthesis of the nanoparticles. As a model, silver nanoparticles **Ag@DT** (DT = dodecanethiol), with a diameter size of 2.6 ± 0.7 nm, were first prepared following a methodology previously described for gold nanoparticles,[19] consisting in a two-phase system (water-toluene) reduction of $AgNO_3$ by sodium borohydride in the presence of dodecanethiol and tetraoctylammonium bromide as phase-transfer agent (entry 1, Table 1). When the same conditions were applied to EugenolSH, **2**, as stabilizer bulk silver was formed. Then, we assayed the same conditions but using a mixture of dodecanethiol and **2** (1:1) as stabilizers obtaining once again bulk silver. Finally, we succeeded with a monophasic system THF/H_2O as reaction medium. Thus, silver nanoparticles **Ag@EugenolSH** were prepared by reducing an aqueous/THF solution of $AgNO_3$ with 3.2 mol-equiv. of $NaBH_4$ in the presence of the stabilizer **2** (Scheme 4a, entry 2 in Table 1). Similarly, spherical and well dispersed **Ag@TAMSH (**3.2 ± 0.7 nm) were synthesized under these monophasic conditions (Scheme 4b, entry 3 in Table 1). In all cases, transmission electron microscopy images confirmed the presence of small Ag NPs and their diameter could be calculated. Typical Plasmon resonance bands of Ag NPs could be observed in UV-vis spectra of resulting materials (405-461 nm in $CHCl_3$, Table 1, see supplementary information (S18-S23-S28-S30)).

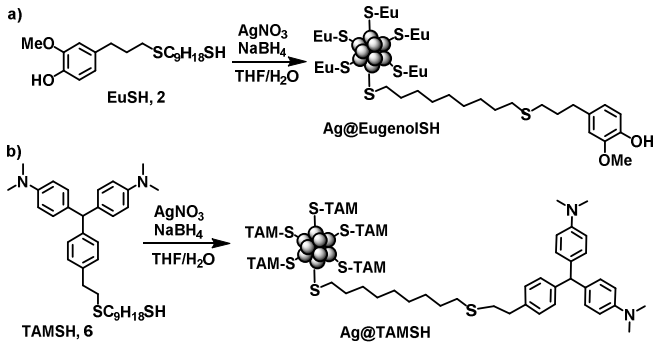

Scheme 4. a) Preparation of **Ag@EugenolSH. b)** Preparation of **Ag@TAMSH**

In order to confirm that the obtained materials did not contain free thiol ligands, NMR DOSY experiments were performed (see SI). A diffusion coefficient of D = $3.98.10^{-10}$ $m^2 \cdot s^{-1}$ for **Ag@EugenolSH** in $CDCl_3$ was observed**,** but not trace of signals at D = $7.08.10^{-10}$ $m^2 \cdot s^{-1}$ were found, corresponding to free EugenolSH in the same conditions. Similarly, the diffusion coefficient for **Ag@TAMSH** was D = $1.58.10^{-10}$ $m^2 \cdot s^{-1}$ in $CDCl_3$, whereas TAMSH presented a valor of D = $5.01.10^{-10}$ $m^2 \cdot s^{-1}$ and it was neither observed. The self-diffusion coefficients of EugenolSH, **2**, and TAMSH, **6**, were consistent with its relative low volume. The corresponding X-Ray diffraction (XRD) patterns showed a very broad and characteristic[20] (111) peak at θ = 38 from the stable face centered cubic (*fcc)* phase of metallic silver in the two studied cases (**Ag@EugenolSH** and **Ag@TAMSH,** see SI). The chemical oxidation state of silver in Ag composites was ascertained by XPS analysis. The survey scan spectrum of **Ag@EugenolSH** and **Ag@TAMSH** exhibits the presence of C 1*s*, S 2*p*, O 1*s*, and Ag 3*d* core levels. Two similar peaks for both samples, at 368.4 and 374.4 eV, corresponded to Ag 3*d* 5/2 and Ag 3*d* 3/2 binding energies, respectively. The splitting of the 3*d* doublet of Ag is 6.0 eV, indicating the formation of metallic Ag(0) NPs (see supplementary information (S22, S27)).[21] The preparation of Ag NPs using fluoroquinolone **9** as stabilizer failed probably due to its low solubility in the mixture THF/H_2O.

We were also interested in the obtention of Ag@Antibio materials with complementary properties in terms of wettability, thus water-soluble NPs. It has been shown in the literature that compounds bearing poly(ethylene oxide) units, such as polyethylene glycol (PEG), can be used as protecting agents acting as hydrophilic ligands for metal nanoparticles including silver.[22] Encouraged by the results shown in our hands by PEG-tagged derivatives in the formation of metal nanoparticles[23] we sought to create a PEG-antibiotic derivative. Although FQSH, **9**, was not a good precursor for Ag NPs, we selected the fluoroquinolones family because they could be easily modified in order to introduce the poly(oxyethylenated) chain in their structure. This strategy could allow us to have a fluoroquinolone derivate finally linked to Ag. Thus, ethyl 7-chloro-6-fluoro-4-hydroxyquinoline-3-carboxylate was first prepared as previously described in the literature[18] and then it was treated with propargyl bromide in the presence of K_2CO_3/DMF at 90°C for 2h affording **10** in 70% yield. Then, we planned to prepare the PEG-tagged molecule through a "click" [2+3] copper-catalyzed alkyne-azide cycloaddition reaction (CuAAC) on the triple bond.[23] The azide coupling partner was obtained in two steps. Treatment of commercially available MeO-PEG-OH with methanesulfonyl chloride (2 equiv.) in the presence of triethylamine in dichloromethane furnished the corresponding mesylate (77% yield). This was then allowed to react with sodium azide in DMF at 60°C for 24h to afford the corresponding azide in 73% yield (Scheme 5).[23a]

Finally, the copper-catalyzed 1,3-dipolar cycloaddition between alkyne **10** and azide MeO-PEG-N_3 (molar ratio 1:1) under the standard click conditions[24] provided compound **11** (70% yield) which was hydrolyzed to afford the acid **12** in quantitative yield. Silver nanoparticles **Ag@FQPEG** were prepared by reducing an aqueous/THF solution of $AgNO_3$ with .2 equiv. of $NaBH_4$ in the presence of the stabilizer **12** (1 equiv.) (Scheme 5, entry 4 in Table 1). TEM analysis confirmed the formation of spherical and dispersed nanoparticles with a mean size of 11.0 ± 0.5 nm. The lattice fringe spacing measurements indicate that the regular lattice spacing of d = 0.23 nm is consistent with the (*111*) plane in the *fcc* structure of Ag(0). The electron diffraction (ED) pattern evidenced also the other planes (*200*), (*220*) and (*311*) belonging to the *fcc* Ag single crystal.

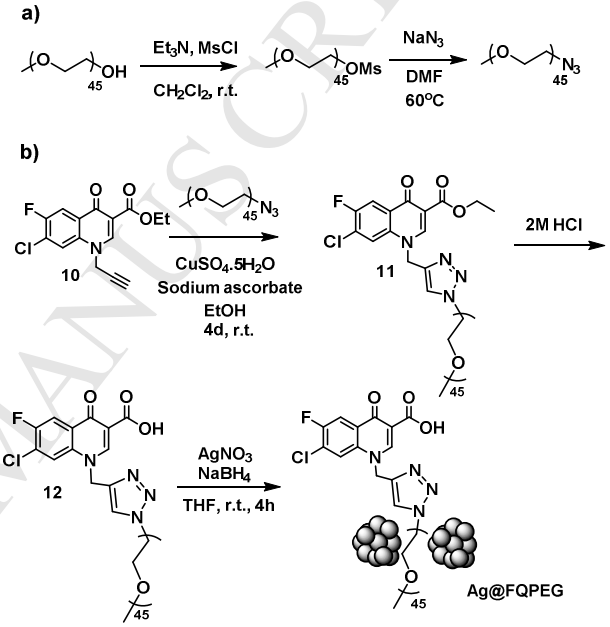

Scheme 5. a) Preparation of MeO-PEG-N_3.b) Preparation of **Ag@FQPEG**

Then, the silver nanoparticles **Ag@DT**, **Ag@EugenolSH**, **Ag@TAMSH** and **Ag@FQPEG** (10^{-3} mmol of Ag(0) in each case, % of Ag in the material was determined in all cases from char yield in TGA experiments, Table 1) were dispersed in THF and applied onto a piece of cotton fabric (3x3 mm) to give **Fabric DT**, **Fabric Eu**, **Fabric TAM** and **Fabric FQPEG** respectively. SEM images of cotton fiber coated and un-coated were carried out. A particulate morphology could be easily observed on the cotton surface after coating (see as example the SEM of **Fabric Eu** in Figure 1).

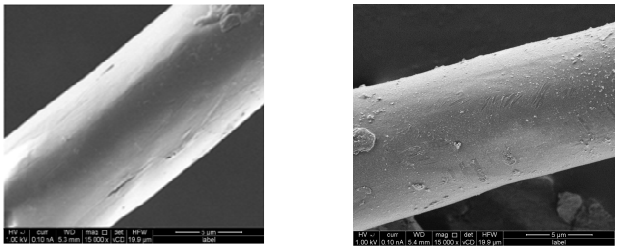

Figure 1. SEM images of cotton fiber. Left: un-coated; Right: **Fabric Eu**

Table 1. Preparation and characteristics of Ag NPs

Entry	Ag NPs	Ag[a] (mmol)	Ag%[b]	λ_{max}[c] (UVVIS)	Diameter (nm) (HRTEM)[d]
1	**Ag@DT**	0.11	61.5	447	2.6 ± 0.7
2	**Ag@EugenolSH**	0.3	31.8	461	2.3 ± 0.2
3	**Ag@TAMSH**	0.3	17.4	452	3.2 ± 0.7
4	**Ag@FQPEG**	0.08	19.8	405	11.0 ± 0.5

[a]$AgNO_3$ mmol; Ag/stabilizer (1:1); [b]calculated from TGA; [c]in $CHCl_3$; [d]200 NPs counted.

The second part of this work was devoted to an assessment of the antibacterial properties of the cotton fabrics. Microbicidal experiments were performed using *Staphylococcus aureus* (*S. aureus*) ATCC 15981 and *Pseudomonas aeruginosa* (*P. aeruginosa*) PAO1 as bacteria. These two strains were chosen to represent Gram-positive and Gram-negative bacteria, respectively. These experiments consisted in transferring 3 different pieces (3x3 mm) of each cloth to a microplate containing 200 µl of the bacterial suspensions at 5 x 10^6 cfu/mL in 25% Luria Bertani (LB). These suspensions were then allowed to incubate in the dark in the presence of the fabrics with a mechanical rotator at 50 rpm at 37°C for 18 h. After incubation, serial dilutions were performed to determine the concentration (cfu/ml) of each bacteria in each well. A blank control of an untreated fabric was used**.** Firstly, we compared the activity of different fabrics for *S. aureus* (Figure 2*).* No bactericidal effect was observed for **Fabric DT** probably due to the hydrophobicity of the long dodecanethiol chains that surrounds the surface of the nanoparticles, avoiding the interaction between Ag NPs and bacteria, and the possible leaching of Ag(I) cations to the solution. Best bactericidal performance was obtained for **Fabric TAM**, with a decrease of 3 log units. This fabric is coated with hydrophilic Ag NPs stabilized by TAMSH, which possess two tertiary amines that will be at least partially protonated in the aqueous medium. This last result is in concordance with the fact that surface charge is a deterministic factor. This antimicrobial enhancement of **Fabric TAM** could be possible due to the positive charge of the capping agents on the Ag surface, which facilitates a strong ionic interaction between the Ag NPs and the negatively-charged bacteria membrane.[25] This effect has been described before by using Ag NPs stabilized by a cationic surfactant, such as an hyper-branched poly(amidoamine) with terminal dimethylamino groups (PAMAM-N(CH_3)$_2$).[26] In addition, a decrease of the bacterial colonies per mL up to at least 1.4 log units for the **Fabric Eu** and 2 orders of magnitude for **Fabric FQPEG** was observed**.** In the case of **Ag@FQPEG**, a part of the intrinsic effect of the fluoroquinolone moiety, the water solubility of the Ag NPs would enhance the release of this antibacterial agents from the textile to the suspension of bacteria improving the microbicidal activity. Finally, we can conclude that spherical Ag NPs with similar size but different protecting agents (entries 1,2 and 3 of Table 1) gave extremely different microbicidal results.

Then, we centred our studies on the microbicidal experiments using the *P. aeruginosa* PAO1 as bacteria (Figure 3). The experiments were repeated as described above for *S. aureus*. Once again, no bactericidal effect was observed for **Fabric DT**. Furthermore, **Fabric TAM**, in contrast with the results obtained for *S. aureus*, was not active in this case. On the other hand, **Fabric Eu**, coated with neutral **Ag@EugenolSH**, causes a bacterial decrease of 1.6 log units showing the effect of the presence of eugenol. The different antibacterial performance of these Ag-Antibio NPs is probably due to the intrinsic effect of the antibiotic moiety. In addition, a decrease of up to at least 1.5 log units for **Fabric FQPEG** is obtained, which is indicative of the effect of fluoroquinolone. In addition, we consider that the water solubility of the **Ag@FQPEG** would also enhance the release of the antibacterial agents from the textile to the suspension of bacteria improving the microbicidal activity.

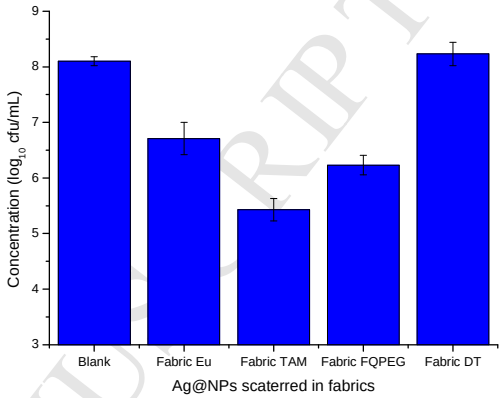

Figure 2. Effect of coated fabrics on the *S. aureus* cultures.

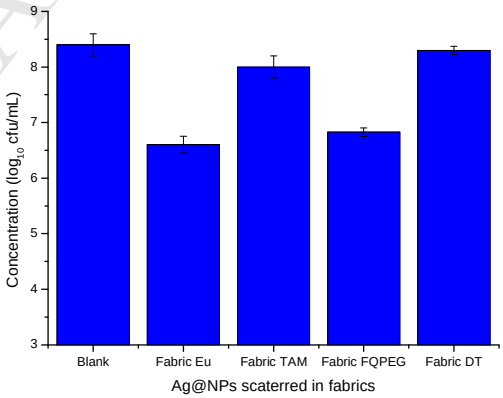

Figure 3. Effect of coated fabrics on the *P. aeruginosa* cultures.

3. Conclusions

As a conclusion, several silver-antibiotic nanoparticles have been prepared using microbicidal derivatives as stabilizers. Surface coating of these Ag NPs resulted to be an essential factor in their antimicrobial activity. Antibacterial tests showed that **Fabric DT** coated with hydrophobic **Ag@DT** do not show antibacterial activity. However, textiles coated with more hydrophilic Ag NPs present activity against Gram-negative or Gram-positive bacteria. Best bactericidal performance was obtained for **Fabric TAM** with a bacterial decrease of 3 log units for the *S. aureus* strain. **Ag@TAMSH** can interact with bacteria with different mechanisms; the presence of partially positive ammonium salts in the surface of the nanoparticles probably enhances their antimicrobial effects towards *S. aureus*. In addition, a decrease of the bacterial colonies per mL up to at least 1.4 log units for the **Fabric Eu** and 2 orders of magnitude for **Fabric FQPEG** was observed**.** With respect to *P. aeruginosa* strain, **Fabric Eu** and **Fabric FQPEG** also showed good antimicrobial activity. Furthermore, in the case of **Ag@FQPEG**

we consider that the water solubility of the Ag NPs would also enhance the release of the antibacterial agents from the textile to the suspension of bacteria improving the microbicidal activity. These antimicrobial fabrics could be applied in all type of medical textiles as gauzes and bandages.

4. Experimental section

4.1. Materials and methods

All of the reagents were purchased from commercial suppliers and used without purification. Solvents were dried prior use. Melting points were measured in a bloc Kofler apparatus from Reichert or in a B-545 apparatus from Büchi and are uncorrected. ^{1}H NMR spectra were recorded on a 400 and 360 MHz spectrometer in deuterated chloroform. ^{13}C NMR spectra were recorded using a 63 and 90 MHz spectrometer. High-resolution mass spectrometry (HRMS) was performed on a Q-TOF spectrometer with micromass MS software using electrospray ionization (ESI).

4.2. Synthetic procedures

*1.1. 4-(3-((9-mercaptononyl)thio)propyl)-2-methoxyphenol, **2** (EugenolSH)*

In a 25 mL round bottom flask, eugenol, **1**, (0.50 g, 3.0 mmol, 1 eq.), dodecane-1,12-dithiol (1.3 mL, 9.0 mmol, 3 eq.) and 6 mL of glycerol were added. The mixture was warmed up to 80^{o}C and let stirring for 3h. Extractions were done with Et_2O and water. Then, the organics were dried and evaporated. The resulting crude was purified by a chromatographic column using as eluent a mixture of 2:1 (Hex:Et_2O), affording 0.76 g (85% yield) of **2** as a white solid; **m. p.:** 78.5-79.2^{o}C; **n_{max} ATR (υ, cm^{-1}):** 3429 (OH), 2919, 1602, 1524, 1240; **d_H (250 MHz CDC1$_3$)** 6.84 (d, *J* = 8.2 Hz, ArH, 1H), 6.71 – 6.66 (m, ArH, 2H), 5.57 (s, O<u>H</u>, 1H), 3.88 (s, OC<u>H</u>$_3$, 3H), 2.66 (t, *J* = 7.5 Hz, C_{Ar}-C<u>H</u>$_2$, 2H), 2.58 – 2.46 (m, C<u>H</u>$_2$SC<u>H</u>$_2$, C<u>H</u>$_2$SH, 6H), 1.88 (quint, *J* = 7.5 Hz, C<u>H</u>$_2$CH$_2$S, 2H), 1.60 (m, SCH$_2$C<u>H</u>$_2$, C<u>H</u>$_2$CH$_2$SH, 4H), 1.44 – 1.25 (m, -(C<u>H</u>$_2$)$_5$-, SH, 11H); **d_C (63 MHz, CDCl$_3$)** 147.3, 144.6, 134.4, 121.9, 115.1, 111.9, 56.8, 35.4 , 34.9, 33.0, 32.3, 32.3, 30.6, 32.3, 30, 29.9, 29.8, 29.2, 25.5; **HRMS (ESI+):** MH$^+$, found 379.1733. $C_{19}H_{32}O_2S_2$ requires 379.1736.

*1.2. 4,4'-((4-vinylphenyl)methylene) bis(N,N-dimethylaniline), **5***

In a 10 mL Schlenk flask under Ar atm, 4-vinylbenzaldehyde (0.5 g, 3.8 mmol, 1 eq.), *N*,*N*-dimethylaniline (1.4 mL, 11.4 mmol, 3 eq.) and $NbCl_5$ (0.1 g, 0.4 mmol, 0.1 eq.) were added. The mixture was warmed up to 120 ^{o}C and let stirring for 4 h. A chromatographic column (Hex:Et_2O, 8:1) was performed, affording 0.77 g of **5** (57% yield) as a yellow oil; **d_H (360 MHz, CDCl$_3$)** 7.35 (d, *J* = 8.1 Hz, ArH, 2H), 7.14 (d, *J* = 8.1 Hz, ArH, 2H), 7.02 (d, *J* = 8.8 Hz, ArH, 4H), 6.73 (dd, *J* = 17.6, 10.9 Hz, C<u>H</u>=CH$_2$, 1H), 6.71 (d, *J* = 8.8 Hz, ArH, 4H), 5.73 (d, *J* = 17.6 Hz, CH=C<u>H</u>$_2$, 1H), 5.40 (s, C<u>H</u>(Ph)$_3$, 1H), 5.22 (d, *J* = 10.9 Hz, CH=C<u>H</u>$_2$, 1H), 2.95 (s, C<u>H</u>$_3$, 12H). **d_C (91 MHz, CDCl$_3$)** 149.9, 146.2, 137.7, 136.1, 133.6, 130.9, 130.4, 126.9, 113.9, 113.5, 55.7, 41.7.

*1.3. 9-((4-(bis(4-(dimethylamino)phenyl)methyl)phenethyl)thio) nonane-1-thiol, **6** (TAMSH)*

In a 25 mL round bottom flask, 4,4'-((4-vinylphenyl)methylene)bis(*N*,*N*-dimethylaniline) (0.63 g, 0.2 mmol, 1 eq.), 6 mL of glycerol and nonane-1,9-dithiol (1.13 mL, 0.5 mmol, 3 eq.) were added. The mixture was warm up to 60 ^{o}C and let stirring overnight. After cooling, extractions with H_2O and CH_2Cl_2 were done (3 x 3 mL). The organics were dried and evaporated. A chromatographic column with a gradient of Hex:Et_2O (8:1) to Et_2O was performed, affording 0.21 g (22% yield) of **6** as a colorless oil; **n_{max} ATR (υ, cm^{-1}):** 2922, 2851, 1594, 1515, 1358, 808, 630. ; **d_H (250 MHz CDC1$_3$)** 7.16 – 7.06 (m, ArH, 4H), 7.01 (d, *J* = 8.7 Hz, ArH, 4H), 6.69 (d, *J* = 8.7 Hz, ArH, 4H), 5.38 (s, C<u>H</u>(Ph)$_3$, 1H), 2.94 (s, C<u>H</u>$_3$, 12H), 2.89 – 2.72 (m, PhCH$_2$C<u>H</u>$_2$, 4H), 2.55 (m, SC<u>H</u>$_2$, C<u>H</u>$_2$SH, 4H), 1.61 (m, SCH$_2$C<u>H</u>$_2$, C<u>H</u>$_2$CH$_2$SH, 4H), 1.38 (m, (CH$_2$)$_5$, SH**,** 11H); **d_C (63 MHz, CDCl$_3$)** 148.9, 143.4, 138.0, 132.8, 129.8, 129.3, 128.1, 112.4, 54.6, 40.7, 36.0, 33.9, 33.6, 32.2, 29.6, 29.3, 29.1, 28.9, 28.8, 28.3, 24.5; **HRMS (ESI+):** MH$^+$, found 549.3326. $C_{34}H_{48}N_2S_2$ requires 549.3332.

*1.4. 7-chloro-6-fluoro-1-(3-((9-mercaptononyl)thio)propyl)-4-oxo-1,4-dihydroquinoline-3-carboxylate, **8***

In a 10 mL round bottom flask, *ethyl 1-allyl-7-chloro-6-fluoro-4-oxo-1,4-dihydroquinoline-3-carboxylate* (0.65 g, 2.1 mmol, 1 eq.), nonane-1,9-dithiol (0.91 mL, 4.2 mol, 2 eq.) and 40 mL of glycerol were added. The mixture was warmed up to 110^{o}C and let stirring overnight. Then, extractions with CH_2Cl_2 and H_2O were done, the organics were dried and evaporated. The crude mixture was purified by a chromatographic column (9:1 Et_2O:CH_2Cl_2), obtaining 0.20 g (35% yield) of a yellowish solid, characterized as **8**; **m.p.:** 152-154 ^{o}C; **n_{max} ATR (υ, cm^{-1}):** 3095, 2987, 1693, 1607, 1549, 1527, 1290; **d_H (360 MHz CDC1$_3$)** 8.50 (s, NHC<u>H</u>, 1H), 8.19 (d, $J_{H\text{-}F}$ = 9.0 Hz, ArH, 1H), 7.67 (d, $J_{H\text{-}F}$ = 5.7 Hz, ArH, 1H), 4.42 – 4.27 (m, C<u>H</u>$_2$CH$_3$, NC<u>H</u>$_2$, 4H), 2.60 - 2.48 (m, C<u>H</u>$_2$SC<u>H</u>$_2$, C<u>H</u>$_2$SH, 6H), 2.15 (quint, *J* = 7.2 Hz, C<u>H</u>$_2$CH$_2$S, 2H), 1.64 – 1.53 (m, SCH$_2$C<u>H</u>$_2$, C<u>H</u>$_2$CH$_2$SH, 4H), 1.39 – 1.22 (m, CH$_2$C<u>H</u>$_3$, (C<u>H</u>$_2$)$_5$, S<u>H</u>, 14H); **d_C (90 MHz, CDCl$_3$)** 172.6, 164.9, 155.3 (d, $J_{C\text{-}F}$ = 252,1 Hz, ArC-F), 149.3, 135.3, 129.3 (d, $J_{C\text{-}F}$ = 6.4 Hz, ArC), 127.1 ($J_{C\text{-}F}$ = 20.0 Hz, ArC-Cl), 118.2, 114.1 (d, $J_{C\text{-}F}$ = 22.8 Hz), 110.7, 60.9, 52.2, 33.9, 32.3, 29.4, 29.2, 29.0, 28.9, 28.7, 28.5, 28.2, 27.7, 24.5, 14.3; **HRMS (ESI+):** MNa$^+$, found 524.1459. $C_{24}H_{33}ClFNO_3S_2Na$ requires 524.1467

*1.5. 7-chloro-6-fluoro-1-(3-((9-mercaptononyl) thio) propyl)-4-oxo-1,4-dihydro quinoline-3-carboxylic acid, **9** (FQSH)*

In a 100 mL round bottom flask, 25 mL of a 2 M HCl solution was added over 0.2 g (0.4 mmol) of fluoroquinolone **8**. The mixture was warmed up to reflux and let stirring overnight. Then, the mixture was cooled down to r.t. and extractions with chloroform were done. The organic phases were dried and evaporated affording 0.18 g (100% yield) of a yellowish solid, identified as the organic carboxylic acid **9**; **m.p.:** 183-184 ^{o}C; **n_{max} ATR (υ, cm^{-1}):** 3437 (OH), 2923, 2851, 1613, 1518, 1348; **d_H (250 MHz CDC1$_3$)** 8.88 (s, NHC<u>H</u>,1H), 8.21 (d, $J_{H\text{-}F}$ = 8.5 Hz, ArH, 1H), 7.93 (d, $J_{H\text{-}F}$ = 5.6 Hz, ArH, 1H), 4.52 (bs, NC<u>H</u>$_2$, 2H), 2.66 - 2.46 (m, C<u>H</u>$_2$SC<u>H</u>$_2$, C<u>H</u>$_2$SH, 6H), 2.21 (bs, C<u>H</u>$_2$CH$_2$S, 2H), 1.72 – 1.49 (m, SCH$_2$C<u>H</u>$_2$, C<u>H</u>$_2$CH$_2$SH, 4H), 1.44 – 1.20 (m, (C<u>H</u>$_2$)$_5$, SH, 11H); **d_C (90 MHz, CDCl$_3$)** 177.1, 166.3, 155.7 (d, $J_{C\text{-}F}$ = 253.7 Hz, ArC-F), 149.0, 135.9, 129.1 (d, $J_{C\text{-}F}$ = 20.5 Hz, ArC-Cl), 126.5 (d, $J_{C\text{-}F}$ = 6.6 Hz, ArC$_5$), 119.2, 113.2 (d, $J_{C\text{-}F}$ = 23.0 Hz, ArC), 108.6, 53.2, 33.9, 32.3, 29.3, 29.2, 29.0, 28.8, 28.7, 28.5, 28.3, 28.2, 28.1, 24.5; **HRMS (ESI+):** MNa$^+$, found 496.1154. $C_{22}H_{29}ClFNO_3S_2Na$ requires 496.1157.

*1.6. Ethyl 7-chloro-6-fluoro-1-((1-(2-methoxy-PEG)-1H-1,2,3-triazol-4-yl)methyl)-4-oxo-1,4-dihydroquinoline-3-carboxylate, **11**.*

In a 50 mL Schlenk flask under argon atmosphere, the alkyne **10** (0.2 g, 0.62 mmol, 1 eq.), the PEG-N_3 (1.26 g, 0.62 mmol), sodium ascorbate (0.06 g, 0.31 mmol, 0.5 eq.), $CuSO_4 \cdot 5H_2O$ (0.06 g, 0.25 mmol, 0.4 eq.) and 10 mL of EtOH were added. The

reaction was stirred at room temperature over 4 days. Once the reaction was over, it was poured into water an extractions with dichloromethane were done. After evaporation, 1.12 g (70% yield) of an orange solid was obtained, identified as **11**; **m.p.:** 195-197 ^{o}C; **n_{max} ATR (υ, cm^{-1}):** 2885, 1722, 1612, 1466, 1239, 1100; **d_H (250 MHz CDC1$_3$)** 8.71 (s, 1H, Ar), 8.21 (d, *J* = 10.8 Hz, ArH, 1H), 7.98 (s, 1H, C=CH-N, 1H), 7.95 (d, *J* = 7.2 Hz, ArH, 1H), 5.49 (bs, NCH$_2$C=C, 2H), 4.52 (t, *J* = 5.0 Hz, NCH$_2$CH$_2$, 2H), 4.37 (q, *J* = 7.2 Hz, OCH$_2$CH$_3$, 2H), 3.56 (bs, (CH$_2$)$_n$, 232H), 3.38 (s, OCH$_3$, 3H), 1.42 (t, *J* =7.2 Hz, OCH$_2$CH$_3$, 3H); **MALDI-TOF:** 2264.64 ($n_{average}$ = 43).

*1.7. 7-Chloro-6-fluoro-1-((1-(2-methoxy-PEG)-1H-1,2,3-triazol-4-yl)methyl)-4-oxo-1,4-dihydroquinoline-3-carboxylic acid, **12***

In a 100 mL round bottom flask, 25 mL of a 2 M HCl solution was added over 0.21 g (0.1 mmol) of fluoroquinolone **11**. The mixture was warmed up to reflux and let stirring overnight. Then, the mixture was cooled down to r.t. and extractions with chloroform were done. The combined organic phases were dried and evaporated affording 0.19 g (100% yield) of a solid identified as the carboxylic acid **12**; **m.p.:** 201-203 ^{o}C; **n_{max} ATR (υ, cm^{-1}):** 3437 (OH), 2923, 2851, 1613, 1518, 1348; **d_H (250 MHz CDC1$_3$)** 14.56 (s, OH, 1H), 9.12 (s, ArH, 1H), 8.40 (d, *J* = 5.8 Hz, ArH, 1H), 8.21 (m, ArH, 2H), 5.68 (bs, NCH$_2$C=C, 2H), 4.54 (t, *J* = 5.0 Hz, NCH$_2$CH$_2$, 2H), 3.56 (bs, (CH$_2$)$_n$, 268H), 3.37 3.38 (s, OCH$_3$, 3H); **MALDI-TOF:** 2264.64 ($n_{average}$ = 43).

1.8. General procedure for the preparation of the silver nanoparticles

In a 250 mL erlenmeyer, 0.3 mmol (1 equiv.) of the corresponding stabilizer in 50 mL of THF and a solution of $AgNO_3$ (0.049 g, 0.3 mmol, 1 eq.) in 6 mL of water were added. Over this mixture, a previous prepared solution of $NaBH_4$ (0.036 g, 0.9 mmol, 3.2 mol-equiv.) was added dropwise. The mixture was let stirring during 3h at room temperature. After this period, part of the THF was evaporated. Then, chloroform was added, the phases were separated, and the organic fraction washed with water. Finally, the organics were dried with Na_2SO_4 and evaporated. The resulting dark red solid was washed with cold diethyl ether, obtaining silver NPs.

Bibliography

1. (a) Zhou, H.; Wang, H.; Niu, H.; Gestos, A.; Lin, T. *Adv. Func. Mater*. **2013**, *23*, 1664-1670; (b) Liu, Y.; Liu, Z.; Liu Y.; Hu. H.; Li, Y.; Yan, P.; Yu, B.; Zhou, F. *Small* **2015**, *11*, 426-431; (c) Wang, H.; Xue, Y.; Ding, J.; Feng, L.; Wang, X.; Lin, T. *Angew. Chem. Int. Ed*. **2011**, *50*, 11433-11436.
2. (a) Wang, L.; Zang, X.; Li, B.; Sun, P.; Yang, J.; Xu, H.; Liu, Y. *ACS Appl. Mater. Interfaces* **2011**, *3*, 1277-1281.
3. (a) Chen, S; Li, X.; Li, Y.; Sun, J. *ACS Nano* **2015**, *9*, 4070-4076; Li, Y.-C.; Mannen, S.; Morgan, A. B.; Chang, S.; Yang, Y.-H.; Condon, B.; Grulan J. C. *Adv. Mater.* **2011**, *23*, 3926-3931.
4. *A Search for Antibacterial Agents*, Chapter 4: *Antibacterial Modification of Textiles using Nanotechnology*, V. Bobbarala Ed., IntechOpen, Rijeka, Croatia, 2012.
5. For reviews on silver as antibacterial agent see: (a) Zheng, K.; Setyawati, M. I.; Leong, D. T.; Xie, J. *Coord. Chem. Rev.* **2018**, *357*, 1-17; (b) Chernousova, S.; Epple, M. *Angew. Chem. Int. Ed.* **2013**, *52*, 1636-1653; (c) Morones, J. R.; Elechiguerra, J. L.; Camacho, A.; Holt, K.; Kouri, J. B.; Ramírez, J. T.; Yacaman, M. J. *Nanotechnology*, **2005**, *16*, 2346-2353.
6. (a) Xue, C.-H.; Chen, J.; Yin, W.; Jia, S.-T., Ma, J.-Z. *Applied Surface Science*, **2012**, *258*, 2468-2472; (b) Wu, M.; Ma, B.; Pan, T.; Chen, S.; Sun, J. *Adv. Func. Mater*. **2016**, *26*, 569-576; (c) Eremenko, A. M.; Petrik, I. S.; Smirnova, N. P.; Rudnko, A. V.; Marikvas, Y. S. *Nanoscale Res. Lett.*, **2016**, *11*, 1-9.
7. Morones, J. R.; Elechiguerra, J. L.; Camacho, A.; Holt, K.; Kouri, J. B.; Ramırez, J. T.; Yacaman, M.J., *Nanotechnology*, **2005**, *16*, 2346-2353.
8. Simoncic B.; Tomsic, B. *Textile Research Journal*, **2010**, *80*, 1720-1737; Monge, M. *An. Quim.* **2009**, *105*, 33-41.
9. Devi, L. S.; Joshi, S. R. *Microbiology*, **2012**, *40*, 27-34.
10. (a) Niembro, S.; Vallribera, A.; Moreno-Mañas, M. *New J. Chem.* **2008**, *32*, 94-98; (b) Niembro, S.; Shafir, A.; Vallribera, A.; Alibés, R. *Org. Lett.* **2008**, *10*, 3215-3218; *Synfacts*, **2008**, 1228; (c) Berini, R.; Cacchi, S.; Fabrizi, G.; Niembro, S.; Prastaro, A.; Shafir, A.; Vallribera, A. *ChemSusChem* **2009**, *2*, 1031-1040; (d) Berini, R.; Cacchi, S.; Fabrizi, G.; Forte, G.; Petrucci, F.; Prastaro, A.; Niembro, S.; Shafir, A; Vallribera, A. *Org. Biomol. Chem.* **2009**, *7*, 2270-2273; (e) Berini, R.; Cacchi, S.; Fabrizi, G.; Forte, G.; Petrucci, F.; Prastaro, A.; Niembro, S.; Shafir, A.; Vallribera, A. *Green Chem.* **2010**, *12*, 150-158; (f) Niembro, S.; Shafir, A. Vallribera, A. *Arkivoc* **2010**, (iii), 181-190; (g) Boffi, A.; Cacchi, S.; Pierpaolo, C.; Cirilli, R.; Fabrizi, G., Prastaro, A.; Niembro, S. ; Shafir, A., Vallribera, A. *ChemCatChem* **2011**, *3*, 347-353; (h) Niembro, S.; Donnici, S.; Shafir, A.; Vallribera, A. Buil, L. B.; Esteruelas, M. A.; Larramona, C. *New J. Chem.* **2013**, *37*, 278-282; (f) Martín, L.; Molins, A.; Vallribera, A. *New J. Chem.* **2016**, *40*, 10208-10212; (i) Santacruz, L.; Niembro, N.; Santillana, A.; Shafir, A.; Vallribera, A. *New J. Chem.* **2014**, *38*, 636-640.
11. Toh, H. S.; Batchelor-Mcauley, C.; Tschulik, K.; Compton R. G. *Science China Chemistry*, **2014**, *57*, 1199-1210.
12. Lenardao, E. J.; Jacob, R. G.; Mesquita, K. D.; Lara, R. G.; Webber, R.; Martínez, D. M.; Savegnago, L.; Mendes, S. R.; Alves, D. G.; Perin, G. *Green Chem. Lett. Rev*. **2013**, *6*, 269-276.
13. Kalemba, D.; Kunicka, A. *Curr. Med. Chem*. **2003**, *10*, 813-829.
14. Srivastava, S.; Sinha, R.; Ro, D. *Aquatic Toxicology*, **2004**, *66*, 319–329.
15. Molander, G. A.; Brown, A. R. *J. Org. Chem.* **2006**, *71*, 9681-9686.
16. Hou, J.-T.; Gao, J.-W.; Zhang**,** Z.-H. *Monatsh. Chem.* **2011,** *142*, 495-499.
17. Leyva, S. Leyva, E. *Bol. Soc. Quim. Mex.* **2008**, *2*, 1-13.
18. Koga, H.; Itoh, A.; Murayame, S.; Suzue, S.; Irikura, T. *J. Med. Chem.* **1980**, *23*, 1358-1363.
19. Brust, M., Walker, M., Bethell, D., Schiffrin, D. J., Whyman, R. *J. Chem. Soc., Chem. Commun.*, **1994**, 801-802.
20. C.-H.Xue, J. Chen, W. Yin, S.-T. Jia, J.-Z. Ma, Appl. Surf. Sc. 2012, 258, 2468-2472.
21. Liang, M.; Su, R.; Huang, R.; Qi, W.; Yu, Y.; Wang, L.; He, Z. *ACS Appl. Mater. Interfaces*, **2014**, *6*, 4638-4649.
22. (a) Liu, G.; Li, Kaijun; Luo, Quanquing, Wang, H.; Zhang, Z. *J. Colloid Interf. Sci*., **2017**, *490*, 642-651; (b) Ganji, N.; Khan, I. A.; Bothum, G. D. *Langmuir*, **2018**, *34*, 2039-2945.
23. (a) Pd NP: Mejías, N.; Pleixats, R.; Shafir, A.; Medio-Simón, M.; Asensio, G. *Eur. J. Org. Chem.* **2010**, 5090-5099; (b) Rh NP: Guo, W.; Pleixats, R.; Shafir, A.; Parella, T. *Adv. Synth. Catal*. **2015**, *357*, 89-99; (c) .Au NP: Guo, W.; Pleixats, R.; Shafir, A. *Chem. Asian J*. **2015**, *10*, 2437-2443.
24. Kumar, R.; Sathaiah, G.; Shekhar, A. C.;. Raju, K.; Rao, P. S.; Shanthan, P.; Narsaiah, B.; Raju, Y. K.; Murthy, U. S. N. *J. Heterocyclic Chem.*, **2015**, *52*, 235-242.
25. (a) Gottenbos, Grijpma, D. W.; van der Mai, H. C.; Feijen, J. Busscher, H. J. *J. Antimicrob Chemother* **2001**, *48*, 7-13; (b) Abbaszadegan, A.; Ghahramani, Y; Gholami, A.; Hemmateenejad, B.; Dorostkar, S.; Nabavizadeh, M.; Sharghi, H. *J. Nanomater*. **2015**, 1-8.
26. Zhang, Y.; Peng, H.; Huang, W.; Zhou, Y; Yan, D. *J. Colloid Interface Sci* **2008**, *325*, 371-376.

Acknowledgments

We are thankful for financial support from Spain's MICINN (CTQ2014-53662-P) and MEC (CTQ2016-81797-REDC) and DURSI-Generalitat de Catalunya (2017 SGR 465 and 2017 SGR 1726).

Supplementary Material

Supplementary material of this article is available including NMR, IR spectra and ESI of new compounds 2, 6, 8, 9, 11 and

Click here to remove instruction text...

12; and UV-vis, IR, DOSY, TEM, TGA, DSC, XRD, EDX and XPS of Ag NPs.